ISSN 1067-8212, Russian Journal of Non-Ferrous Metals, 2025, Vol. 66, No. 1, pp. 17–23. © Pleiades Publishing, Ltd., 2025.

The Effect of Gd Addition on Mechanical Properties and Microstructure Evolution during Hot Deformation of β-Solidified γ-TiAl Based Alloy

V. S. Sokolovsky[a], * (ORCID: 0000-0001-5607-2765), P. V. Panin[b], and G. A. Salishchev[a] (ORCID: 0000-0002-0815-3525)

[a] *Belgorod State University, Belgorod, 308015 Russia*

[b] *Federal State Unitary Enterprise "All-Russian Scientific Research Institute of Aviation Materials" (National Research Center "Kurchatov Institute"—VIAM), Moscow, 105005 Russia*

**e-mail: sokolovskiy@bsuedu.ru*

Received May 6, 2025; revised May 19, 2025; accepted May 19, 2025

Abstract—The effect of Gd microalloying on the microstructure, mechanical behavior, and structural evolution during hot deformation in the ($\alpha_2 + \gamma$) phase field has been investigated on two experimental β-solidifying alloys based on γ–TiAl – Ti–45Al–2V–1Nb–1Zr and Ti–45Al–2V–1Nb–1Zr–0.2Gd (at %). The addition of Gd led to a reduction in the average size of plate-like ($\alpha_2 + \gamma$) colonies from 250 to 140 μm, and the inter-lamellar spacing decreased from 160 to 110 nm in the as-cast state. It was shown that the reduction in the average colony size resulted in a decrease in the yield strength and peak stresses during hot deformation, with this effect being more pronounced at lower deformation temperatures. Additionally, the introduction of Gd resulted in the fraction of recrystallized/spheroidized volume increase of the forming α_2/γ-phase grains/particles and also their size reduction.

Keywords: intermetallics, TiAl, REE, microalloying, workability

DOI: 10.1134/S1067821225600498

HIGHLIGHTS

- Gd microalloying led to grain refinement of lamellar colonies in as-cast condition
- Yield strength and peak stress decrease at hot deformation with Gd alloying
- Recrystallized/spheroidized grain fraction increases from 50 to 65% with Gd alloying
- Gd improves ductility and hot workability of β-solidified γ-TiAl alloy

1. INTRODUCTION

Intermetallic alloys based on γ-TiAl are promising materials for application in aviation, space, and automotive industries due to their high specific strength, heat resistance, and oxidation resistance at elevated temperatures [1–3]. Unlike traditional titanium and nickel-based superalloys, γ-TiAl-based alloys possess significantly lower density, making them attractive for use in aircraft engine components, automotive turbines, and other parts operating at temperatures up to 800°C. This can substantially improve the efficiency and operational characteristics of power plants [4, 5]. However, low plasticity and labor-intensive pressure processing of TiAl alloys, which could enhance their property balance, limit the application of intermetallic alloys [6–8]. During hot deformation of cast alloys in the ($\alpha_2 + \gamma$) phase field, the greatest challenges arise, including high flow stresses, deformation localization, and surface cracking in workpieces [8]. The primary reasons for this are the natural brittleness of intermetallic alloys, their low thermal conductivity, high chemical activity (tendency to interact with atmospheric gases at elevated temperatures), and almost unchanged strength reduction upon temperature increase from room to processing level.

It is known that the optimal combination of mechanical properties of intermetallic TiAl alloys (low-temperature plasticity, strength, fracture toughness, creep resistance) is achieved when they have a fine-grained lamellar-type structure with grain size (lamellar colonies) of 150 μm or less. The formation of the required grain size can be achieved via microalloying with modifiers, in particular boron, carbon, and rare earth elements (REEs) [9–14]. Microalloying with REEs is one of the promising directions for improving the mechanical properties and technological efficiency of γ-TiAl-based alloys [15, 16]. It is known that the addition of REEs leads to alloy modification, refinement of their structure, and, as a result,

improves mechanical characteristics, particularly plasticity [16]. REEs have a high affinity for oxygen which promotes the formation of dispersed oxide particles. These particles act as effective obstacles to dislocation movement during creep and limit grain growth during crystallization, thermomechanical and thermal treatments [16, 17]. Previous studies have shown that alloying with REEs such as Y, La, Gd, Sc, and Ce improves creep resistance and strength characteristics of γ-TiAl-based alloys [15, 16, 18–26]. Alloying with REEs results in significant refinement of lamellar colonies in the cast state [22].

Literature data on the influence of REEs (La and Y) on mechanical behavior and microstructure evolution demonstrate nonlinear dependencies of alloy properties on their content. In [24], a comparative study was conducted on the effect of microalloying with REEs on the microstructure and properties of the Ti–43.5Al–4Nb–1Mo–0.1B[1] alloy with varying La content from 0.1 to 0.5 at %. The authors found that at a La content of 0.2 at %, a large number of oxide particles (~2 μm in size) are formed resulting in maximum flow stresses during deformation and a slowdown in the kinetics of dynamic recrystallization/spheroidization processes of the lamellar structure during hot deformation. At higher REE contents, particle size increases, as does their volume fraction, leading to a reduction in colony size and flow stress during deformation. In [20], a non-monotonic variation in the strength and ductility of the Ti–47Al alloy was observed with the increasing *Y* content: at <0.5 at % *Y* the yield strength and relative elongation increase, while at >0.5 at % Y both properties decrease. This behavior is related to changes in the morphology of Al_2Y particles: at <0.5 at % Y the phase consists of small particles, but as *Y* content increases, a continuous network forms along the boundaries of lamellar colonies, leading to embrittlement of the alloy. In [27], it was noted that the size of recrystallized/spheroidized grains/particles decreased after hot deformation above the eutectoid transformation temperature in the Ti–43Al–9V–0.3Y and Ti–45Al–5Nb–0.3Y alloys compared to the Ti–43Al–9V and Ti–45Al–5Nb alloys, respectively. The authors attribute the decrease in grain/particle size to REE-enriched particles that suppress their growth during dynamic recrystallization.

Thus, it is known that REE alloying effectively reduces the size of lamellar colonies, positively influencing mechanical behavior during hot deformation by increasing alloy ductility and reducing flow stresses. However, there is a dependence on the morphology, dispersion, and volume fraction of REE-enriched phases. One such element is Gd [15, 28], whose addition leads to minimal colony sizes in the as-cast state even at contents of 0.15–0.2 at % due to limited diffusion in the melt and the formation of more dispersed particles, which are less prone to eutectic colony formation. Furthermore, the influence of Gd alloying on microstructure evolution during hot deformation has not been previously investigated. In this work, the effect of Gd microalloying on mechanical behavior and structural evolution during hot deformation in the upper part of the ($\alpha_2 + \gamma$)-phase field has been studied using the Ti–45Al–2V–1Nb–1Zr and Ti–45Al–2V–1Nb–1Zr–0.2Gd alloys as examples.

2. MATERIALS AND METHODS

The ingots ∅70 × 350 mm of experimental Ti–45Al–2V–1Nb–1Zr and Ti–45Al–2V–1Nb–1Zr–0.2Gd alloys were obtained using a double vacuum arc remelting process followed by vacuum induction melting. To study the microstructure, a scanning electron microscope (SEM) (FEI Nova Nano SEM 450) was employed. Images were taken in the diffraction mode of backscattered electrons at an accelerating voltage of 30 kV. Studies on mechanical behavior and microstructure evolution of the alloys within the ($\alpha_2 + \gamma$) phase field (T = 1000, 1050, 1100°C; strain rate 0.001 s^{-1}) were conducted using cylindrical samples with dimensions of ∅10 × 15 mm. Tests were performed on an Instron 300LX universal testing machine (force of 30 tons for static tests) equipped with a furnace for sample heating. The samples were placed in the heated furnace, held at test temperature for 10 min, and then compressed under different strain rates until a true strain of 1.2 was reached. After completing the tests, the samples were quenched in water. For further microstructure analysis, the deformed samples were cut into two parts along the deformation axis. The volume fraction of recrystallised/spheroidised particles was determined from SEM images and calculated as the ratio of the area occupied by recrystallised/spheroidised particles to the total area multiplied by 100% using Digimizer software tools.

3. RESULTS

The microstructure of Ti–45Al–2V–1Nb–1Zr and Ti–45Al–2V–1Nb–1Zr–0.2Gd alloys in the cast state is shown in Fig. 1. The alloys have a fully lamellar structure with a colony size of 250 μm in the Gd-free alloy and 140 μm in the Gd-doped alloy (Figs. 1a, 1c). The average inter-lamellar spacing was 110 and 160 nm in the alloy with and without Gd, respectively (Figs. 1b, 1d). Also, in both alloys particles of the γ-phase up to 5 μm in size and 1–2% volume fraction were present along the colony boundaries (Figs. 1a, 1c). Gd alloying led to the formation of Gd_2O_3 oxide particles [14] and $GdAl_3$ aluminides [7], located predominantly along the colony boundaries (Fig. 1c). The size of these particles ranged from 0.1 to 5 μm, and their volume fraction did not exceed 1.5%.

[1] Hereinafter chemical compositions of alloys are given in atomic percent (at %).

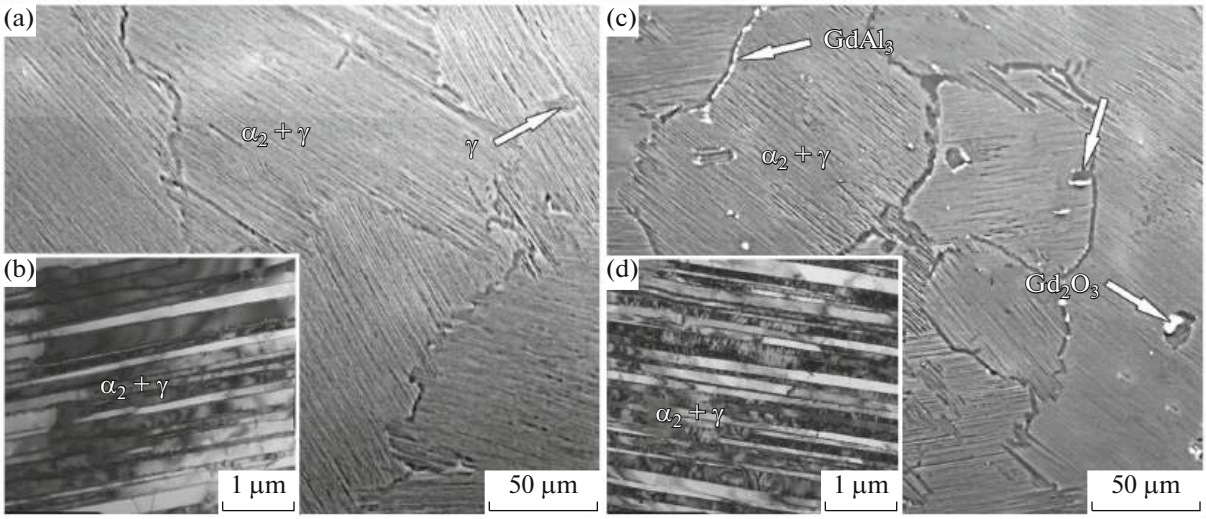

Fig. 1. Microstructures of as-cast Ti–45Al–2V–1Nb–1Zr and Ti–45Al–2V–1Nb–1Zr–0.2Gd alloys ((a, b) SEM; (c, d) TEM).

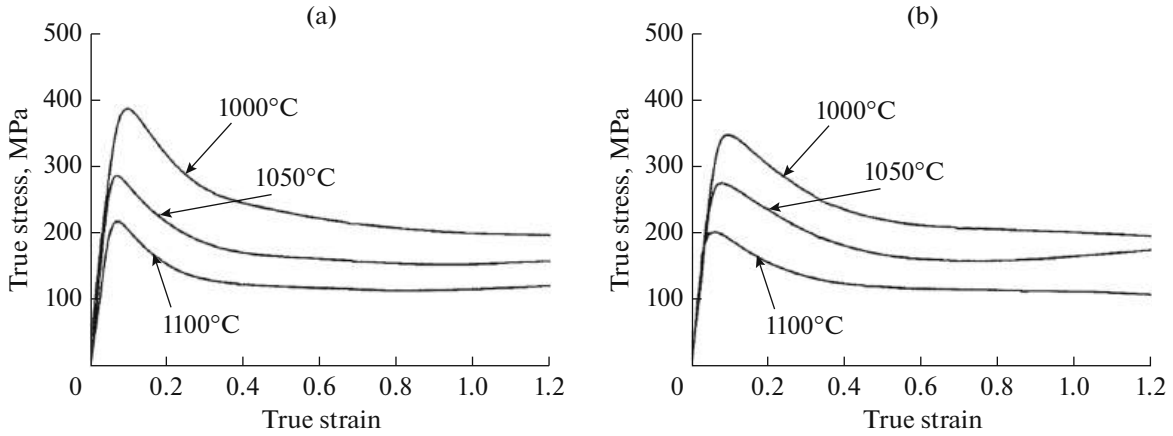

Fig. 2. Stress-strain curves for as-cast (a) Ti–45Al–2V–1Nb–1Zr and (b) Ti–45Al–2V–1Nb–1Zr–0.2Gd alloys obtained during compression at $T = 1000–1100$°C and strain rate 0.001 s^{-1}.

The alloy specimens were subjected to uniaxial compression testing within the temperature range of 1000–1100°C at an initial strain rate of 0.001 s^{-1}. Figure 2 presents the stress-strain curves for the studied alloys.

At the initial stage, strain hardening was observed in both alloys up to $e = 0.05–0.1$ at all test temperatures (Figs. 2a, 2b). As the degree of strain increased, intense softening occurred, leading to the onset of steady-state flow (Fig. 2). A comparison of the curves for both alloys reveals that Gd addition reduces the yield strength and peak stresses; however, the stresses during the steady-state stage are approximately equal (Table 1, Figs. 2a, 2b). This observation is likely related to the smaller size of lamellar colonies in the as-cast state (Fig. 1). On the lateral surfaces of the Gd-free alloy samples, cracks were detected across the entire temperature range after testing. In contrast, no cracks were observed in the Gd-containing alloy samples after deformation above $T = 1050$°C.

Table 1. Yield strength of as-cast Ti–45Al–2V–1Nb–1Zr and Ti–45Al–2V–1Nb–1Zr–0.2Gd alloys

Deformation temperature	Ti–45Al–2V–1Nb–1Zr	Ti–45Al–2V–1Nb–1Zr–0.2Gd
1000°C	431 MPa	351 MPa
1050°C	313 MPa	277 MPa
1100°C	222 MPa	205 MPa

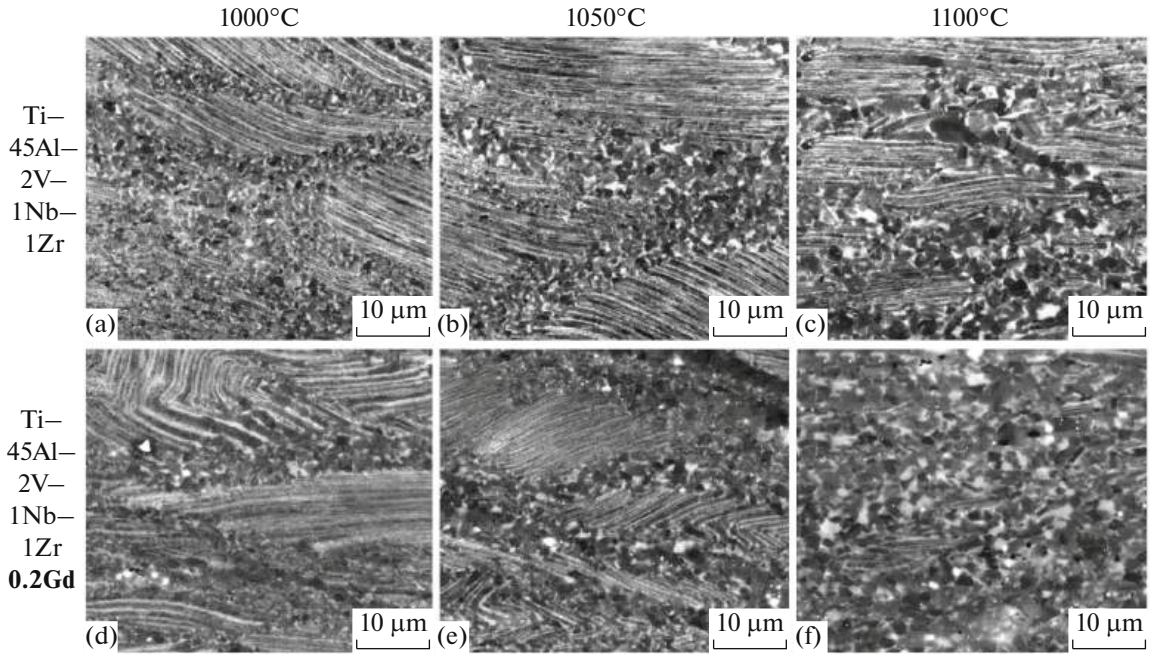

Fig. 3. Microstructures of Ti–45Al–2V–1Nb–1Zr (a–c) and Ti–45Al–2V–1Nb–1Zr–0.2Gd (d–f) alloys after compression tests at $T = 1000–1100$°C (strain rate 0.001 s^{-1}, $e = 1.2$). The loading direction is vertical in all cases.

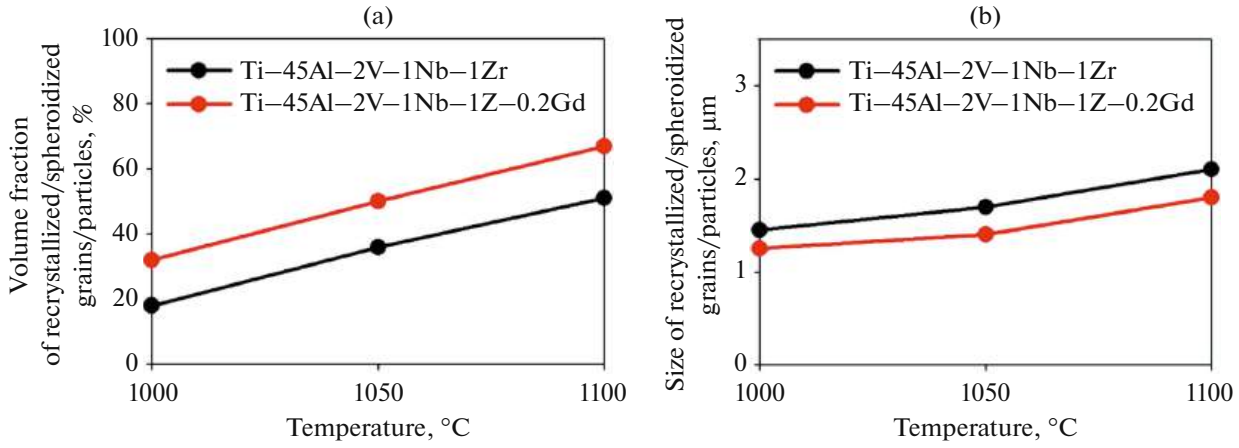

Fig. 4. Dependences of (a) the volume fraction and (b) size of recrystallized/spheroidized grains/particles on the deformation temperature for Ti–45Al–2V–1Nb–1Zr and Ti–45Al–2V–1Nb–1Zr–0.2Gd alloys.

The microstructures of deformed alloy samples at $e = 1.2$ deformation at temperatures of 1000, 1050, and 1100°C, with a strain rate of 0.001 s^{-1}, are presented in Fig. 3. The microstructures of both alloys after uniaxial compression testing were characterized by the elongation of lamellar colonies perpendicular to the loading axis (Fig. 3). The processes of spheroidization and dynamic recrystallization occurred during deformation, resulting in the formation of equiaxed grains/particles of the α_2- and γ-phases along the boundaries of lamellar colonies. An increase in deformation temperature led to an enhancement in the volume fraction of recrystallized grains/particles in both cases (Figs. 3, 4). It is evident that spheroidization and dynamic recrystallization were more pronounced in the Gd-containing alloy, likely due to the smaller colony size (Fig. 1), which facilitated greater deformation homogeneity. However, it should be noted that further increases in deformation temperature could intensify oxidation processes, potentially negatively impacting the surface quality of the compressed samples.

Figure 4a shows the dependence of the volume fraction of recrystallized/spheroidized grains/particles on deformation temperature for the alloys. With an increase in deformation temperature, there was a rise in the volume fraction of recrystallized/spheroidized

grains/particles, reaching approximately 65% in the Gd-containing alloy after deformation at 1100°C. The volume fraction of recrystallized/spheroidized grains/particles in the Gd-free alloy also increased with temperature but it did not exceed 50% even at 1100°C. The size of the recrystallized/spheroidized grains/particles was slightly smaller in the case of the Gd-containing alloy (Fig. 4b). With an increase in deformation temperature from 1000 to 1100°C, the grain/particle size grew from 1.3 to 2 μm, respectively (Fig. 4b).

4. DISCUSSION

The obtained results demonstrate that Gd microalloying has a significant influence on the initial microstructure, mechanical behavior, and structural evolution of γ-TiAl-based alloys during hot deformation in the upper area of the $(\alpha_2 + \gamma)$ phase field. The primary effects include a reduction in flow stresses, an increase in the fraction of recrystallized/spheroidized structure, as well as improved ductility. Additionally, it can be assumed that the stress drop in the temperature range of 1050–1100°C occurs due to the acceleration of the $\alpha_2(D0_{19}) \rightarrow \alpha(A3)$ phase disordering process at temperatures above 1100°C [29]. These results are consistent with previous studies on the effects of REEs in γ-TiAl-based alloys [24, 27, 30].

The investigation into the effects of Gd addition on the structure and mechanical behavior revealed that doping it into the alloy leads to a refinement of the as-cast structure, reducing colony sizes from 250 to 140 μm. Additionally, Gd microalloying reduces peak stresses during hot deformation by 80–20 MPa, increases the volume of recrystallized/spheroidized structures by 15%, and decreases the tendency of the alloy to form surface cracks. The primary cause of such effects is likely the reduction in lamellar colony size and inter-lamellar spacing in the as-cast state. The application of other REEs (La and Y) requires higher concentrations (>0.3 at %) to achieve similar reductions in flow stresses [24, 27]. This behavior is attributed to Gd being more effective in producing finer colonies in the as-cast state by forming a large number of uniformly distributed Gd-rich particles which suppress grain growth [15]. It should be noted that the reduction in inter-lamellar spacing from 160 to 110 nm is not significant and such changes have little impact on ductility and/or flow stress [31], even at room temperature [32].

A smaller size of initial lamellar colonies leads to an increase in boundary length, resulting in more active dynamic recrystallization/spheroidization [33]. This behavior exhibits as an increased fraction of recrystallized/spheroidized grains/particles and improved structural homogeneity after deformation [27, 30]. The authors [30] also note more active dynamic recrystallization and delocalization of deformation, which was attributed to the smaller size of lamellar colonies in the initial state. Besides that, Gd addition results in a retardation of $\alpha_2 \rightarrow \gamma$ phase transformation, expressed as reduced inter-lamellar spacing [34]. This fact may lead to the formation of recrystallized/spheroidized grains/particles of smaller size [7], which was observed in Y-alloyed materials [27, 30].

The obtained results show that Gd microalloying is an effective method for improving the deformability of γ-TiAl-based alloys; when using La or Y to achieve the same effect, their content needs to be increased by 1.5 times [20, 24, 27].

CONCLUSIONS

(1) A study was conducted on the microstructure of the cast alloys Ti–45Al–2V–1Nb–1Zr and Ti–45Al–2V–1Nb–1Zr–0.2Gd. The addition of Gd led to grain refinement, characterized by a reduction in the average size of lamellar colonies from 250 to 140 μm and inter-lamellar spacing from 160 to 110 nm. This refinement is attributed to the formation of Gd-rich particles and the slowing down of the $\alpha_2 \rightarrow \gamma$ transformation kinetics.

(2) The effect of Gd alloying on mechanical behavior and structural evolution during hot deformation in the upper $(\alpha_2 + \gamma)$ phase field was investigated. It has been established that Gd alloying results in a decrease in yield strength and peak stresses, along with an increase in the fraction of recrystallized/spheroidized grains/particles from 50 to 65% at $T = 1100$°C. This alloying also leads to a reduction in grain size and enhanced ductility, as indicated by the absence of cracks at temperatures above 1000°C. These improvements are expected to positively impact the alloy workability during pressure and cutting processes.

(3) Gd microalloying of β-solidified γ-TiAl based alloy resulted in improved workability in the upper $(\alpha_2 + \gamma)$ phase field.

FUNDING

The authors gratefully acknowledge the financial support from the Russian Science Foundation Grant no. 19-79-30066 (https://rscf.ru/en/project/23-79-33001/). The work was carried out using the equipment of the Joint Research Centre of Belgorod State National Research University "Technology and Materials."

CONFLICT OF INTEREST

The authors of this work declare that they have no conflicts of interest.

REFERENCES

1. Appel, F., Paul, J.D.H., and Oehring, M., *Gamma Titanium Aluminide Alloys: Science and Technology,* Wein-

heim: Wiley-VCH, 2011.
https://doi.org/10.1002/9783527636204

2. Clemens, H. and Mayer, S., Design, processing, microstructure, and mechanical properties of advanced γ-TiAl based alloys, *Adv. Eng. Mater.,* 2013, vol. 15, pp. 191–215.
https://doi.org/10.1002/adem.201200231
3. Xu, R., Li, M., and Zhao, Y., A review of microstructure control and mechanical performance optimization of γ-TiAl alloys, *J. Alloys Compd.,* 2023, vol. 932, p. 167611.
https://doi.org/10.1016/j.jallcom.2022.167611
4. Genc, O. and Unal, R., Development of gamma titanium aluminide (γ-TiAl) alloys: a review, *J. Alloys Compd.,* 2022, vol. 929, p. 167262.
https://doi.org/10.1016/j.jallcom.2022.167262
5. Bewlay, B.P., Nag, S., Suzuki, A., and Weimer, M.J., TiAl alloys in commercial aircraft engines, *Mater. High Temp.,* 2016, vol. 33, pp. 549–559.
https://doi.org/10.1080/09603409.2016.1183068
6. Chen, X., Tang, B., Liu, D., Wei, B., Zhu, L., Liu, R., Kou, H., and Li, J., Dynamic recrystallization and hot processing map of Ti–48Al–2Cr–2Nb alloy during the hot deformation, *Mater. Charact.,* 2021, vol. 179, p. 111332.
https://doi.org/10.1016/j.matchar.2021.111332
7. Sokolovsky, V.S., Stepanov, N.D., Zherebtsov, S.V., Nochovnaya, N.A., Panin, P.V., Zhilyakova, M.A., Popov, A.A., and Salishchev, G.A., Hot deformation behavior and processing maps of B and Gd containing β-solidified TiAl based alloy, *Intermetallics,* 2018, vol. 94, pp. 138–151.
https://doi.org/10.1016/j.intermet.2018.01.004
8. Kong, Y., Chen, D., and Zhang, S., High temperature deformation behavior of Ti–46Al–2Cr–4Nb–0.2Y alloy, *Mater. Sci. Eng., A,* 2012, vol. 539, pp. 107–114.
https://doi.org/10.1016/j.msea.2012.01.066
9. Wang, X., Luo, R., Liu, F., Zhu, F., Song, S., Chen, B., Zhang, X., Zhang, J., and Chen, M., Characterization of Gd-rich precipitates in a fully lamellar TiAl alloy, *Scr. Mater.,* 2017, vol. 137, pp. 50–54.
https://doi.org/10.1016/j.scriptamat.2017.04.038
10. Li, W., Inkson, B., Horita, Z., and Xia, K., Microstructure observations in rare earth element Gd-modified Ti–44 at. % Al, *Intermetallics,* 2000, vol. 8, pp. 519–523.
https://doi.org/10.1016/S0966-9795(99)00156-9
11. Prasath Babu, R., Vamsi, K.V., and Karthikeyan, S., On the formation and stability of precipitate phases in a near lamellar γ-TiAl based alloy during creep, *Intermetallics,* 2018, vol. 98, pp. 115–125.
https://doi.org/10.1016/j.intermet.2018.04.017
12. Li, W. and Xia, K., Kinetics of the α grain growth in a binary Ti–44Al alloy and a ternary Ti–44Al–0.15Gd alloy, *Mater. Sci. Eng., A,* 2002, vols. 329–331, pp. 430–434.
https://doi.org/10.1016/S0921-5093(01)01617-3
13. Panin, P.V., Zavodov, A.V., and Lukina, E.A., Effect of thermal exposure on microstructure evolution and mechanical properties of cast beta-solidifying TiAl-based alloy doped with Gd, *Intermetallics,* 2022, vol. 145, p. 107534.
https://doi.org/10.1016/j.intermet.2022.107534
14. Panin, P.V., Kochetkov, A.S., Zavodov, A.V., and Lukina, E.A., Effect of Gd addition on phase composition, structure, and properties of beta-solidifying TiAl-based alloy with Zr and Cr content variability, *Intermetallics,* 2020, vol. 121, p. 106781.
https://doi.org/10.1016/j.intermet.2020.106781
15. Liu, C., Xia, K., and Li, W., The comparison of effects of four rare earth elements additions on structures and grain sizes of Ti–44Al alloy, *J. Mater. Sci.,* 2002, vol. 37, pp. 1515–1522.
https://doi.org/10.1023/A:1014900325485
16. Songbo, Y., Effect of minor Sc on high-temperature mechanical properties of Ti–Al based alloys, *Mater. Sci. Eng., A,* 2000, vol. 280, pp. 204–207.
https://doi.org/10.1016/S0921-5093(99)00667-X
17. Wu, X., Song, D., and Xia, K., Different tensile and compressive creep behaviors in a fully lamellar Ti–44Al–1Mn–2.5Nb–0.15Gd alloy, *Mater. Sci. Eng., A,* 2002, vol. 331, pp. 821–827.
https://doi.org/10.1016/S0921-5093(01)01631-8
18. Wu, Y. and Hwang, S.K., The effect of yttrium on microstructure and dislocation behavior of elemental powder metallurgy processed TiAl-based intermetallics, *Mater. Lett.,* 2004, vol. 58, pp. 2067–2072.
https://doi.org/10.1016/j.matlet.2003.12.036
19. Kartavykh, A.V., et al., Lanthanum hexaboride as advanced structural refiner/getter in TiAl-based refractory intermetallics, *J. Alloys Compd.,* 2014, vol. 588, pp. 122–126.
https://doi.org/10.1016/j.jallcom.2013.11.017
20. Li, B., Kong, F., and Chen, Y., Effect of yttrium addition on microstructures and room temperature tensile properties of Ti–47Al alloy, *J. Rare Earths,* 2006, vol. 24, pp. 352–356.
https://doi.org/10.1016/S1002-0721(06)60123-3
21. Sokolovsky, V.S., Stepanov, N.D., and Salishchev, G.A., The effect of cellular reaction on mechanical behavior and microstructure, *Intermetallics,* 2025, vol. 179, p. 108653.
https://doi.org/10.1016/j.intermet.2025.108653
22. Chen, Y., Kong, F., Han, J., Chen, Z., and Tian, J., Influence of yttrium on microstructure, mechanical properties and deformability of Ti–43Al–9V alloy, *Intermetallics,* 2005, vol. 13, pp. 263–266.
https://doi.org/10.1016/j.intermet.2004.07.014
23. Yang, C.T. and Koo, C.H., Improving the microstructure and high temperature properties of the Ti–40Al–16Nb alloy by the addition of a minor Sc or La-rich Misch metal, *Intermetallics,* 2004, vol. 12, pp. 235–251.
https://doi.org/10.1016/j.intermet.2003.10.010
24. Hadi, M., Shafyei, A., and Meratian, M., A comparative study of microstructure and high temperature mechanical properties of a β-stabilized TiAl alloy modified by lanthanum and erbium, *Mater. Sci. Eng., A,* 2015, vol. 624, pp. 1–8.
https://doi.org/10.1016/j.msea.2014.11.037
25. Wu, Y., Hagihara, K., and Umakoshi, Y., Influence of Y-addition on the oxidation behavior of Al-rich γ-TiAl alloys, *Intermetallics,* 2004, vol. 12, pp. 519–532.
https://doi.org/10.1016/j.intermet.2004.01.008

26. Chen, Y.Y., Li, B.H., and Kong, F.T., Microstructural refinement and mechanical properties of Y-bearing TiAl alloys, *J. Alloys Compd.,* 2008, vol. 457, pp. 265–269. https://doi.org/10.1016/j.jallcom.2007.03.050

27. Kong, F.T., Chen, Y.Y., and Li, B.H., Influence of yttrium on the high temperature deformability of TiAl alloys, *Mater. Sci. Eng., A,* 2009, vol. 499, pp. 53–57. https://doi.org/10.1016/j.msea.2007.09.093

28. Jin, H.H., Kim, S., Ryu, I.S., Kwon, J., Jung, S., and Chun, Y.B., Microstructural characterization of gadolinium-rich phases in titanium alloys, *Heliyon,* 2024, vol. 10, no. 15, e34935. https://doi.org/10.1016/j.heliyon.2024.e34935

29. Panin, P.V., Lukina, E.A., and Shiryaev, A.A., Temperature–time–transformation diagrams construction for beta-solidifying TiAl-based alloy in as-cast condition, *IOP Conf. Ser.: Mater. Sci. Eng.,* 2021, vol. 1079, p. 062010. https://doi.org/10.1088/1757-899X/1079/6/062010.

30. Chen, Y., Li, B., and Kong, F., Effects of minor yttrium addition on hot deformability of lamellar Ti–45Al–5Nb alloy, *Trans. Nonferrous Met. Soc. China,* 2007, vol. 17, pp. 58–63. https://doi.org/10.1016/S1003-6326(07)60048-X

31. Maruyama, K., Yamamoto, R., Nakakuki, H., and Fujitsuna, N., Microstructure evolution during deformation of TiAl alloys, *Mater. Sci. Eng., A,* 1997, vols. 239–240, pp. 419–423. https://doi.org/10.1016/S0921-5093(97)00612-6

32. Panov, D.O., Sokolovsky, V.S., Stepanov, N.D., Zherebtsov, S.V., Panin, P.V., Volokitina, E.I., Nochovnaya, N.A., and Salishchev, G.A., Effect of interlamellar spacing on strength-ductility combination of β-solidified γ-TiAl based alloy with fully lamellar structure, *Mater. Sci. Eng., A,* 2023, vol. 862, p. 144458. https://doi.org/10.1016/j.msea.2022.144458

33. Sakai, T., Belyakov, A., Kaibyshev, R., Miura, H., and Jonas, J.J., Dynamic and post-dynamic recrystallization under hot, cold and severe plastic deformation conditions, *Prog. Mater. Sci.,* 2014, vol. 60, pp. 130–207. https://doi.org/10.1016/j.pmatsci.2013.09.002

34. Sokolovsky, V.S., Stepanov, N.D., Zherebtsov, S.V., et al., The effect of Gd addition on the kinetics of $\alpha_2 \rightarrow \gamma$ transformation in γ-TiAl based alloys, *Intermetallics,* 2020, vol. 120, p. 106759. https://doi.org/10.1016/j.intermet.2020.106759